


# Investigation of the effect of demagnetization fault at Line Start AF-PMSM with FEM

\*<sup>1</sup>Mustafa Eker, <sup>2</sup>Mustafa Özsoy

<sup>1</sup>Gaziosmanpaşa University, Niksar Vocational School of Technical Sciences, Turkey, [mustafa.eker@gop.edu.tr](mailto:mustafa.eker@gop.edu.tr) 

<sup>2</sup>Gaziosmanpaşa University, Faculty of Engineering and Natural Sciences, Electrical and Electronics Engineering, Turkey, [mustafa.ozsoy@gop.edu.tr](mailto:mustafa.ozsoy@gop.edu.tr) 

## Abstract

In motors containing magnets, irreversible demagnetization failure is one of the factors that negatively affect motor performance. In this study, the traditional Axial Flux Permanent Magnet Synchronous Motor (AF-PMSM) rotor structure was changed and the structure that gained the feature of starting from the line was used. Line Start AF-PMSM with 5.5 kW shaft power has 4 poles and each pole consists of 5 magnets. Demagnetization failure was obtained by the flux values of the magnets in any pole are drawn to zero and virtual demagnetization failure is created at certain rates (20%, 40% and 60%). With FEM, the data of the healthy and faulty motor were obtained. The data are then presented comparatively. Obtained data showed that demagnetization fault in Line Start AF-PMSM negatively affects motor performance, and the results are given in detail in the article. The original aspect of the study is that the demagnetization fault in Line Start AF-PMSM was investigated for the first time with FEM.

**Keywords:** Line start, Axial Flux PMSM, Demagnetization fault, FEM

## 1. INTRODUCTION

Permanent Magnet Synchronous Motor (PMSM) has advantages such as high power-to-weight ratio, high torque-inertia ratio and high efficiency and power factor compared to other motors [1,2]. Therefore, it has been widely used in industry recently, especially in servo systems. PMSMs are produced in different structures. The Axial Flux Permanent Magnet Synchronous Motor (AF-PMSM) structure is one of them. The main advantages of this type of motors are high efficiency, power density, torque density, adjustable and planar air gap, and shape compatibility with working areas[3]. One of the disadvantages of these motors is that they cannot start directly from the network. To overcome this, either high-capability drivers or a change in rotor architecture are needed. With the short-circuit cage to be added to the rotor, they can start directly from the line.

As the usage of PMSMs increases, faults in these motors are encountered more frequently. One of these faults is the demagnetization fault. Demagnetization fault is examined in two basic groups as reversible and irreversible demagnetization fault. Reversible demagnetization failure is explained by the state of restoring the material properties when the motor cools down unless the motor is raised above

a certain level in operating condition [4]. Irreversible demagnetization failure is expressed as the situation in which the property losses in the materials cannot be recovered due to different reasons in the operation of the motor.

In PMSMs, demagnetization failure occurs due to reasons such as high temperature, stator faults or inverter-induced short circuit currents, high stator currents, structural parameters, corrosion, magnet life or damage to the magnet. The sources of these failures can be classified as thermal causes, mechanical stress, or environmental factors [5,6]. The main reason for these faults is mostly armature reaction [7].

For this reason, magnets damaged by demagnetization failure will cause the motor to draw more current to obtain the magnetic flux needed, and therefore cause the temperature to increase further. This temperature increase will cause an increase in demagnetization failure [8–10]. Recently, with the more frequent use of electric motors containing rare-earth-elements, the demagnetization failure that occurs in these motors has started to attract more attention of researchers. There are studies on issues such as the causes of the demagnetization fault and its effects on motor performance, and the prevention of damage to other

\* Corresponding Author

components of the machine by detecting potential damages. In addition to the basic parameters such as current and voltage values of the motor, magnetic flux, frequency, torque ripple, and other parameters of the motor are also considered in these studies to protect motor components [11].

In this study, demagnetization fault that may occur in Line Start AF-PMSM was investigated with FEM. Demagnetization fault was created by setting the magnetic flux value provided by some of the 5 identical magnets in 1 pole to zero. Motor parameters were examined with the FEM for healthy and faulty cases and the results were given comparatively.

## 2. LINE START AF-PMSM

Conventional PMSM motors are produced in different topologies. AF-PMSM is one of these topologies. Research/studies on AF-PMSMs have been increasing in recent years. This situation is caused by advantages such as efficiency in unit volume, higher torque, and power density than other radial flux motors, shape advantages, adjustable air gap [12,13]. Another advantage of the AF-PMSM is that it can be produced in different topologies [14].

Since AF-PMSMs contain magnets, additional hardware/processes are needed to be able to start from the line. High-skilled drivers are among them. Another method is the changes made in the motor architecture. With the short-circuit bars added to the rotors, it is provided to start directly from the line. While these short-circuit bars produce the starting torque until it reaches the synchronous speed, they provide the opportunity to be synchronized again in case of pulled out of synchronism. In this way, the AF-PMSM operates as an asynchronous motor in transient state and as a synchronous motor in steady state. In Figure 1, there is a photograph of the short-circuit bar attached to the AF-PMSM.

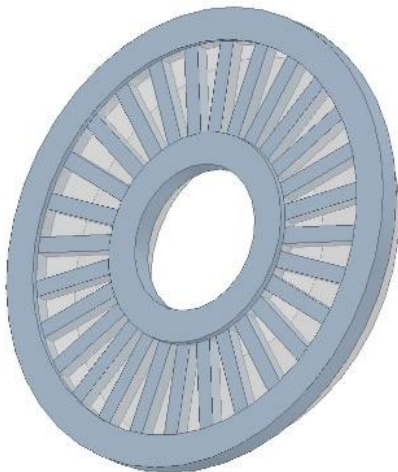


**Figure 1.** Short-circuit bar added to the rotor of the AF-PMSM

In this study, 3-phase 4-pole 5.5kW AF-PMSM was used. Since the rotor structure of the motor used is hybrid, it can start directly from the line. The characteristics and parameters of AF-PMSM are given in Table 1.

**Table 1.** AF-PMSM parameters

Motor parameters	values
Rated voltage (V)	380
Nominal Torque (Nm)	35
Outer/Inner diameter of stator (mm)	248/132
Outer/Inner diameter of rotor with cage (mm)	268/112
Air gap length (mm)	1
Rotor Speed (rpm)	1500
Number of stator/rotor slot	36/28
Stator axial length (mm)	58
Number of stator/rotor slot	36/28
Number of one phase winding (turns)	38
Number of magnets (piece)	20
Magnet thickness/ length (mm)	4/58
Stator material	JFE_20JNEH1500
Core loss coefficient of Stator	
Kh (W/m <sup>3</sup> )	176.316
Kc (W/m <sup>3</sup> )	0.102337
Ke (W/m <sup>3</sup> )	2.72383
Permanent magnet material	N45SH
Squirrel Cage material	Aluminum
Rotor material	Steel 1010

The rotor of the AF-PMSM consists of 4 poles. Since it is a 4-pole structure, there are 2 N and 2 S group magnets. Each magnet group consists of 5 identical magnets. The magnets are mounted on the rotor surface. The magnets used are NdFeB magnets with N45SH code.

## 3. FINITE ELEMENT MODELING

FEM is a solution developed against various engineering problems. In the electrical machine design process, FEM is an effective method to reveal the effects of materials such as core, winding, short-circuit cage, magnet on the motor performance [15]. Ansys software is one of the package programs used to solve these problems. ANSYS Electromagnetics Suite 17.0 software was used in this study. The demagnetization failure of Line Start AF-PMSM was investigated on the full model in 3D environment for 3 main reasons. First, 3D FEM analyzes have higher accuracy than 2D and RMxprt methods. The second reason is that correct results cannot be obtained in 2D resolutions in nonlinear axial flux topology. Since the time parameter is an important factor in FEM analysis, analyzes can be made by taking references such as motor 1/2, 1/3, 1/4, etc. symmetrically in such analyzes. The last reason for the 3D and full model study is the investigation of the demagnetization failure occurring in one of the rotor poles in this study. Because in partial analysis, local faults will give results as if they are spread throughout the motor.

The accuracy of the results obtained in the analysis methods with FEM is directly related to the mesh process to be used. The more nodes used, the higher the accuracy of the result. However, since each node used will prolong the analysis

process, the optimum number of node is selected. The mesh process created varies according to the condition of the motor part. TAU mesh method was used in the analysis. In the ANSYS software, meshing is defined by the number of regions that appear. As a result of the mesh process, 13856 zones were created on the stator, 7000 zones on the rotor, and 3600 zones on the magnets.

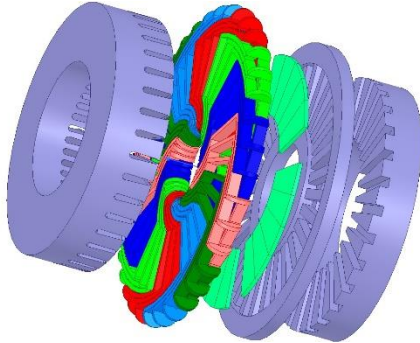


**Figure 2.** Full model of the AF-PMSM at FEM

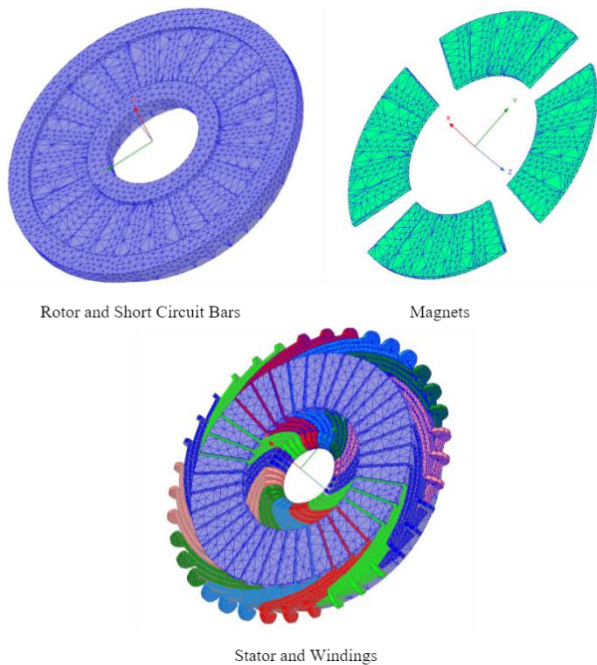


**Figure 3.** Regions formed as a result of meshing applied on AF-PMSM parts

In Figure 2 and Figure 3, the complete model created in the Maxwell software and the images of the regions formed as a result of the applied mesh process are shown. In Figure 4, the generated demagnetization faults are given. The creation of demagnetization in magnets was carried out by pulling the magnetic property of the N45SH material to zero in the material library. In this way, there will be no change in the weight parameter of the material used and its effect on the moment of inertia, which is important for electric motors, will remain constant in all magnets.

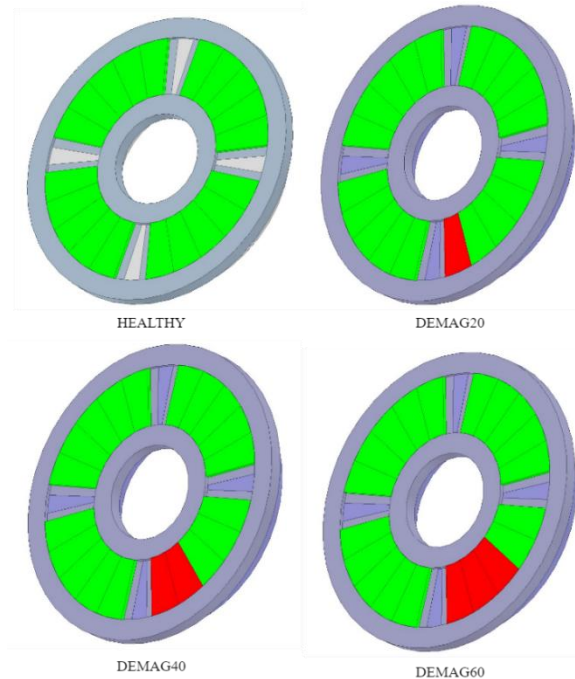


**Figure 4.** The generated demagnetization faults

#### 4. RESULTS AND DISCUSSION

In different fault conditions, the motor was operated for 1.5s with 0.001s time intervals under dynamic operating conditions and parameters such as 3-phase stator current, electromagnetic torque, speed, efficiency, and power factor of the motor were obtained. In Figure 5 and Figure 6, there are phase current graphs of healthy and faulty motors that were dynamically operated for 1.5 seconds at a speed of 1500 rpm at 35 Nm nominal load with FEM in ANSYS Maxwell.

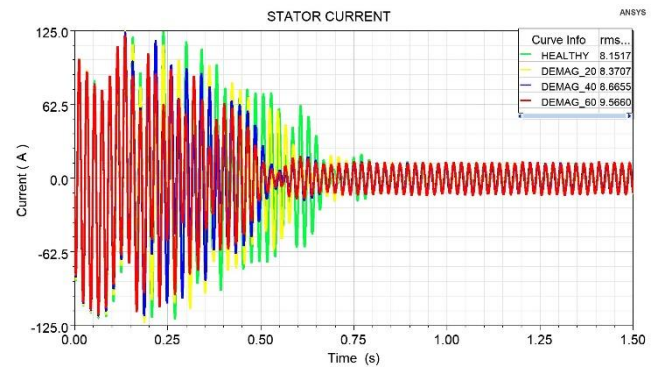


**Figure 5.** Stator one phase current curves of healthy and faulty motors

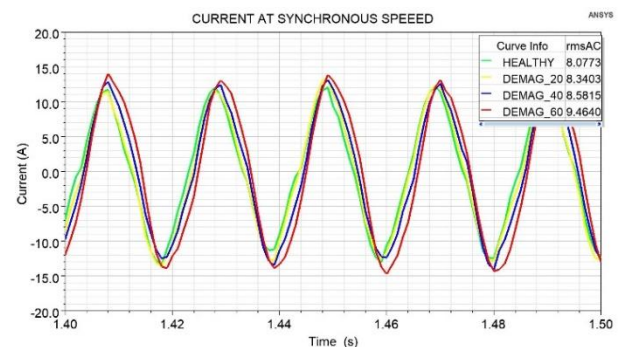


**Figure 6.** Stator one phase current curves of healthy and faulty motors (0.1s)



As a result of the analyzes made with FEM in the graphics, the one phase current rms value was obtained as 8.15 A while the healthy motor was running at nominal load at synchronous speed, and the one phase currents were obtained as 8.37 A, 8.61 A and 9.57 A for 20%, 40% and 60% faulty cases, respectively. When the waveforms are examined in detail, it is observed that as the failure rate increases, the maximum value of the current amplitude increases in the current waveform and there are very small shifts in the period.

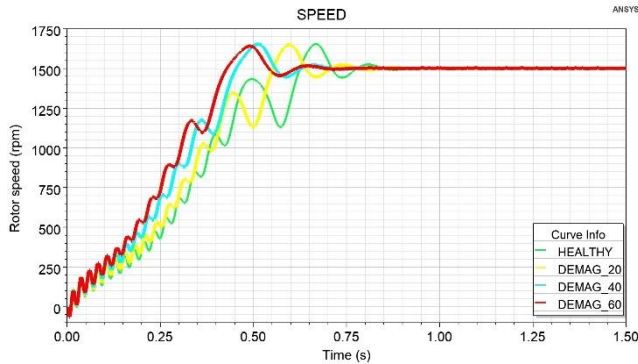


**Figure 7.** Speed curves of healthy and faulty motors

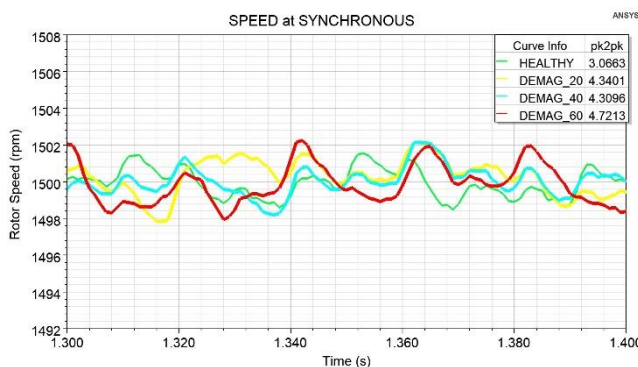


**Figure 8.** Speed curves of healthy and faulty motors (0.1s)

In Figure 7, the speed-time change graph during the starting of the rotor is seen. In Figure 8, the fluctuations in the rotor speed at synchronous speed are seen. It reaches the nominal speed in a time approximately 1.0 second in the analysis of healthy and faulty motors with FEM. It is observed that the motor can reach synchronous speed at full load for all cases. However, as the demagnetization rate increases, the synchronization time becomes shorter, and a decrease is observed in the collapses due to magnets in the acceleration curve. This can be explained by the decrease in the flux provided by the magnets due to the demagnetization failure. It is also observed that the demagnetization failure does not make a change in the acceleration curve at the maximum speed reached. When Figure 8 is examined, it is observed that the fluctuation in speed increases with the increase of demagnetization fault.

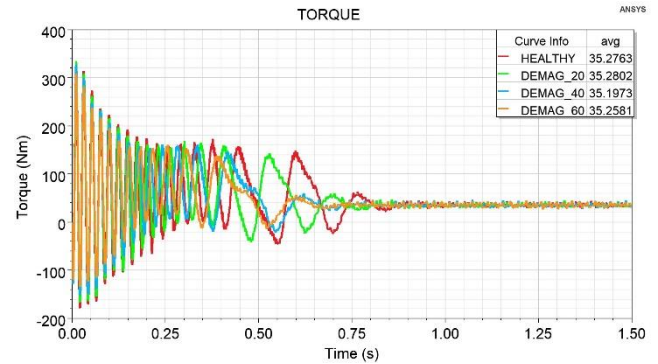


**Figure 9.** Torque curves of healthy and faulty motors

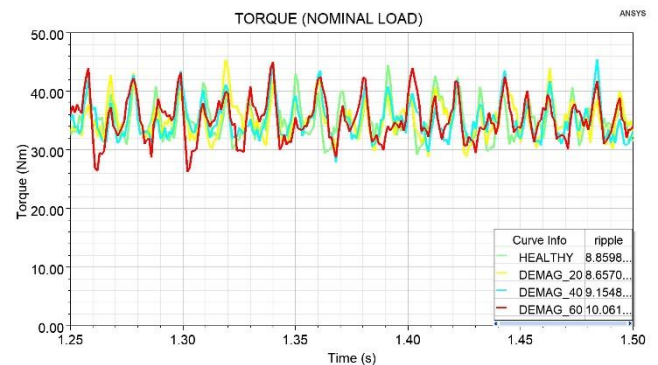


**Figure 10.** Torque curves of healthy and faulty motors (0.25s)

Figure 9 shows the torque curve of the Line Started AF-PMSM during starting. Electromagnetic torque is higher than load torque for both healthy and faulty states until the motor reaches synchronous speed. At the same time, there is a large ripple in electromagnetic torque initially for all situations. The reason for this situation can be said as the reaction of the rotational inertia of the system. Average torque values are positive although there are negative peaks until the electromagnetic torque equals the load torque. In other words, the prototype motor accelerates with positive average torque. The motor reaches the nominal torque value for healthy and faulty situations. The ripple in the torque curve in synchronous operation for these values are given in detail in Figure 10. As the failure rate increases, the torque ripple value occurring at the nominal load value increases. In motor design, one of the factors affecting motor performance is the magnetic flux densities of the materials. The saturation in the motor magnetic materials affects the iron losses in the material and thus the efficiency. The flux densities occurring in the stator and rotor yokes and teeth are also important. In Figure 11 and Figure 12, the magnetic flux density distributions on the stator and rotor, in Figure 13 flux density distributions on magnets are given.

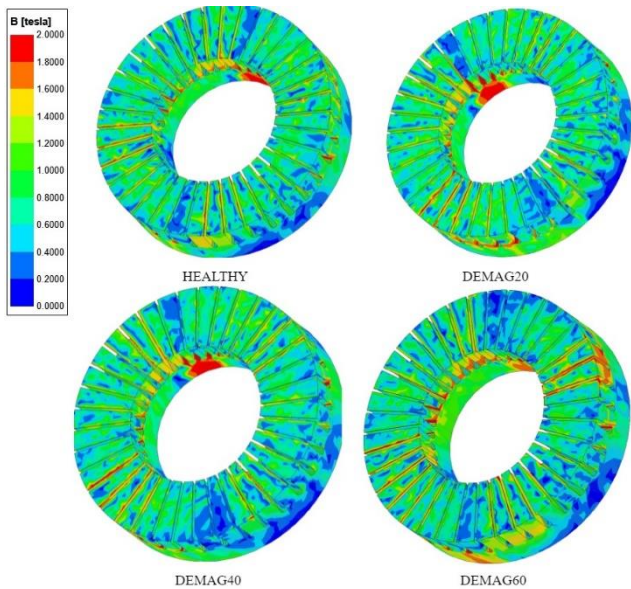


**Figure 11.** Magnetic flux density distributions occurring in the stator

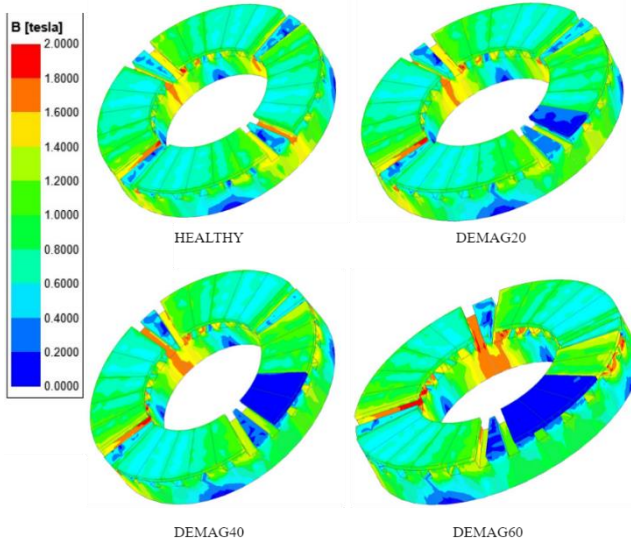


**Figure 12.** Magnetic flux density distributions occurring at rotor

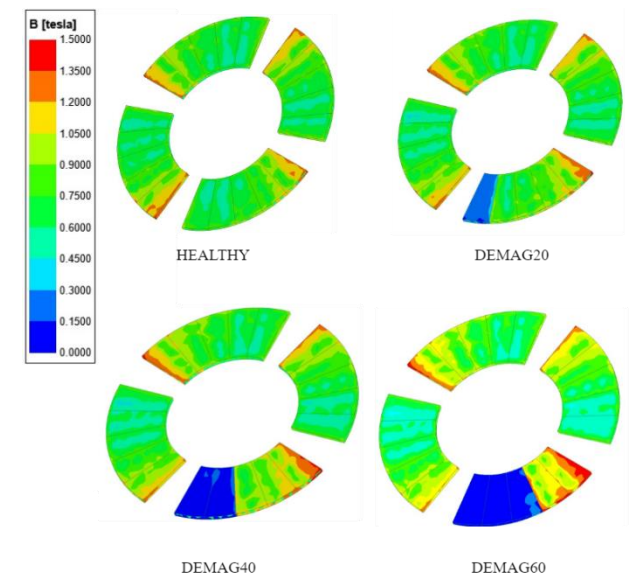


**Figure 13.** Magnetic flux density distributions occurring at magnets

Core losses and magnetization EMF vary directly with the flux density in the teeth, high flux density at these points is undesirable. The flux density in the teeth should not exceed 1.5 T [16]. When the figures are examined, it is seen that the flux distributions in the stator do not change much, but there is a concentration in a certain region with the increase of demagnetization failure. From the flux distributions in the magnets, it is clearly seen that there is an irregularity in the flux distribution due to the demagnetization fault. It shows that higher flux density occurs in healthy magnets in the demagnetized pole, and in this case, healthy magnets may be damaged thermally in long-term operation. While the maximum flux values in the magnets are 1.68 T in a healthy motor, this value reaches 1.83T in a motor with 60% demagnetization failure. This will cause other magnets to demagnetize with temperature in long-term use.

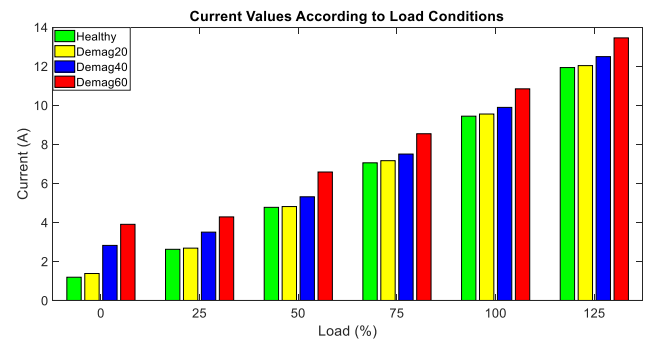


**Figure 14.** Stator current values under different load conditions

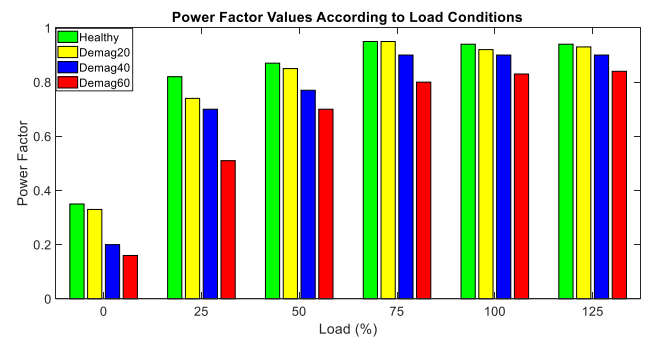


**Figure 15.** Power factor values under different load conditions

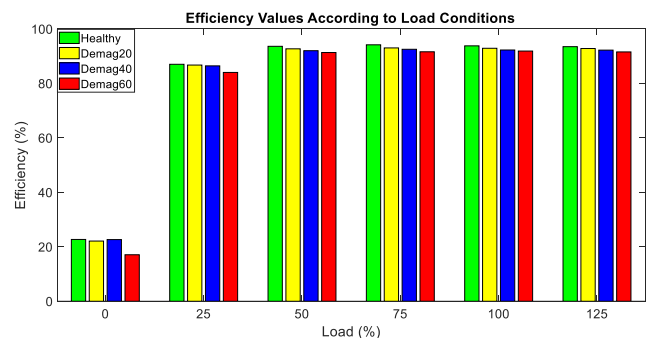


**Figure 16.** Efficiency values under different load conditions

In magnetic analysis, 20%, 40% and 60% demagnetization failures were created at one pole of the motor, and the results obtained under different load conditions were compared with the data obtained from the healthy motor. The data obtained from the faulty motors show that the fault causes changes in the motor current, power coefficient and efficiency parameters. Since  $K_h$ ,  $K_c$  and  $K_p$  values of Steel 1010 steel used in the rotor are not defined in the software used, rotor core losses are not taken into account. As can be seen in Figure 14, it has been observed that the stator current of the motor increases according to the fault rate. Although the increase in the phase current is not obvious when the demagnetization interval is low, this difference is clearly observed when the demagnetization rate of a pole reaches 60%. When Figure 14 -16 is examined, the motor current increases with the increase in the demagnetization fault rate. As the motor current increases, the losses in the motor also increase. In terms of motor efficiency, while the healthy motor runs with 93.79% efficiency at full load, as the ratio of failure increases, the motor runs with approximately 2-3% lower efficiency at the same load (nominal load). In addition, the increase in torque ripple is caused by uneven magnetic pull force and distortions in holding torque. According to the results obtained, it was observed that the demagnetization failure adversely affected the motor performance.

## 5. CONCLUSION

In this study, the effect of demagnetization fault on Line Start AF-PMSM was investigated with FEM. AF-PMSM, that line start feature has been gained by changing the rotor architecture, has a 4-pole 5.5 kW shaft power and is in a single sided structure. One pole of the line start AF-PMSM consists of 5 identical magnets. Demagnetization fault rates of 20%, 40% and 60% are generated in one pole. The results obtained by operating each faulty condition at different loads were compared with the healthy motor. The results showed that demagnetization failure negatively affected the motor parameters. Magnets meet the flux required for excitation in AF-PMSM. With demagnetization failure, the flux provided by the magnets decreases and the motor accordingly draws more current from the network. However, thermal losses increase, power factor decreases, so a decrease in efficiency is observed. It also had negative effects on the speed parameter. The fluctuation at the synchronous speed has increased. While it did not have any negative effect on starting speed due to line start, it caused an increase in starting current. With the demagnetization fault, a 14.4% increase in current, 11.70% in power factor and 2% decrease in efficiency were observed at nominal load. The original aspect of this study is the investigation of demagnetization failure in Line Start AF-PMSM for the first time with FEM.

## ACKNOWLEDGMENTS

This study was supported by the Tokat Gaziosmanpaşa University Scientific Research Projects Unit, Project number 2019/48.

**Author contributions:** Authors equally contributed.

**Conflict of Interest:** Authors declare no conflict of interest.

**Financial Disclosure:** The authors declared that this study has received no financial support.

## REFERENCES

- [1] X. Xiao and C. Chen, 'Reduction of torque ripple due to demagnetization in PMSM using current compensation', *IEEE Trans. Appl. Supercond.*, vol. 20, no. 3, pp. 1068–1071, Jun. 2010.
- [2] M. Fitouri, Y. BenSalem, and M. Naceur Abdelkrim, 'Effects of design variables on demagnetization fault in permanent magnet synchronous motor', *2018 15th Int. Multi-Conference Syst. Signals Devices, SSD 2018*, pp. 71–76, Dec. 2018.
- [3] B. Tian, G. Mirzaeva, Q. T. An, L. Sun, and D. Semenov, 'Fault-Tolerant Control of a Five-Phase Permanent Magnet Synchronous Motor for Industry Applications', *IEEE Trans. Ind. Appl.*, vol. 54, no. 4, pp. 3943–3952, Jul. 2018.
- [4] M. Zhu, W. Hu, and N. C. Kar, 'Torque-Ripple-Based Interior Permanent-Magnet Synchronous Machine Rotor Demagnetization Fault Detection and Current Regulation', *IEEE Trans. Ind. Appl.*, vol. 53, no. 3, pp. 2795–2804, May 2017.
- [5] W. Lu, M. Liu, Y. Luo, and Y. Liu, 'Influencing factors on the demagnetization of line-start permanent magnet synchronous motor during its starting process', *2011 Int. Conf. Electr. Mach. Syst. ICEMS 2011*, 2011.
- [6] R. Dou, F. Song, H. Liu, and X. Men, 'Demagnetization Quantification of PMSM Based on Support Vector Regression', *Proc. - 2018 Progn. Syst. Heal. Manag. Conf. PHM-Chongqing 2018*, pp. 619–623, Jan. 2019.
- [7] Y. Chen, S. Liang, W. Li, H. Liang, and C. Wang, 'Faults and diagnosis methods of permanent magnet synchronous motors: A review', *Applied Sciences (Switzerland)*, vol. 9, no. 10. MDPI AG, p. 2116, May 01, 2019.
- [8] J. X. Shen, P. Li, M. J. Jin, and G. Yang, 'Investigation and countermeasures for demagnetization in line start permanent magnet synchronous motors', *IEEE Trans. Magn.*, vol. 49, no. 7, pp. 4068–4071, 2013.
- [9] Z. Ullah and J. Hur, 'A Comprehensive Review of Winding Short Circuit Fault and Irreversible Demagnetization Fault Detection in PM Type Machines', *Energies*, vol. 11, no. 12, pp. 1–27, 2018, Accessed: Jun. 25, 2021.
- [10] T. Zawilak and M. Gwozdziwicz, 'Demagnetization process in line start permanent magnet synchronous motor', Aug. 2018.
- [11] Z. Ullah, S. T. Lee, M. R. Siddiqi, and J. Hur, 'Online Diagnosis and Severity Estimation of Partial and Uniform Irreversible Demagnetization Fault in Interior Permanent Magnet Synchronous Motor', *2019 IEEE Energy Convers. Congr. Expo. ECCE*

2019, pp. 1682–1686, Sep. 2019.

- [12] M. Aydin, S. Huang, and T. A. Lipo, ‘Torque quality and comparison of internal and external rotor axial flux surface-magnet disc machines’, *IEEE Trans. Ind. Electron.*, vol. 53, no. 3, pp. 822–830, 2006.
- [13] R. Z. Haddad, ‘Detection and Identification of Rotor Faults in Axial Flux Permanent Magnet Synchronous Motors Due to Manufacturing and Assembly Imperfections’, *IEEE Trans. Energy Convers.*, vol. 35, no. 1, pp. 174–183, Mar. 2020.
- [14] A. Parviainen, M. Niemelä, and J. Pyrhönen, ‘Modeling of axial flux permanent-magnet machines’, *IEEE Trans. Ind. Appl.*, vol. 40, no. 5, pp. 1333–1340, Sep. 2004.
- [15] İ. Tarimer, S. Arslan and M. E. Güven, ‘Investigation for Losses of M19 and Amorphous Core Materials Asynchronous Motor by Finite Elements Methods’, *Elektronika Ir Elektrotehnika*, vol. 18, no. 19, pp. 15–18, May. 2012.
- [16] Gürdal, O., *Elektrik Makinalarının Tasarımı*. Bursa Orhangazi University Publications, 518 pp, Bursa2015.